Atmos. Chem. Phys. Discuss., 14, 18541–18589, 2014
www.atmos-chem-phys-discuss.net/14/18541/2014/
doi:10.5194/acpd-14-18541-2014

Atmospheric Chemistry and Physics Discussions
Open Access

Regional climate model assessment of the urban land-surface forcing over central Europe

P. Huszar[1], T. Halenka[1], M. Belda[1], M. Zak[1], K. Sindelarova[1,2], and J. Miksovsky[1]

[1]Department of Meteorology and Environment Protection, Faculty of Mathematics and Physics, Charles University, Prague, V Holešovičkách 2, Prague 8, 180 00, Czech Republic
[2]Laboratoire Atmosphères, Milieux, Observations Spatiales (LATMOS), CNRS, UMR8190, Paris, France

Received: 19 May 2014 – Accepted: 30 June 2014 – Published: 14 July 2014

Correspondence to: P. Huszar (peter.huszar@mff.cuni.cz)

Published by Copernicus Publications on behalf of the European Geosciences Union.

Abstract

For the purpose of qualifying and quantifying the climate impact of cities and urban surfaces in general on climate of central Europe, the surface parameterization in regional climate model RegCM4 has been extended with the Single Layer Urban Canopy Model (SLUCM). A set of experiments was performed over the period of 2005–2009 for central Europe, either without considering urban surfaces or with the SLUCM treatment. Results show a statistically significant impact of urbanized surfaces on temperature (up to 1.5 K increase in summer) as well as on the boundary layer height (increases up to 50 m). Urbanization further influences surface wind with a winter decrease up to $-0.6\,\mathrm{m\,s^{-1}}$, though both increases and decreases were detected in summer depending on the location relative to the cities and daytime (changes up to $0.3\,\mathrm{m\,s^{-1}}$). Urban surfaces significantly reduce evaporation and thus the humidity over the surface. This impacts the simulated summer precipitation rate, showing decrease over cities up to $-2\,\mathrm{mm\,day^{-1}}$. Significant temperature increases are simulated over higher elevations as well, not only within the urban canopy layer. With the urban parameterization, the climate model better describes the diurnal temperature variation, reducing the cold afternoon and evening bias of RegCM4.

Sensitivity experiments were carried out to quantify the response of the meteorological conditions to changes in the parameters specific to the urban environment such as street width, building height, albedo of the roofs and anthropogenic heat release. The results proved to be rather robust and the choice of the key SLUCM parameters impacts them only slightly (mainly temperature, boundary layer height and wind velocity).

Statistically significant impacts are modeled not only over large urbanized areas, but the influence of the cities is also evident over rural areas without major urban surfaces. It is shown that this is the result of the combined effect of the distant influence of the cities and the influence of the minor local urban surface coverage.

1 Introduction

The artificial urban surfaces are clearly distinguished from natural surfaces by mechanical, radiative, thermal and hydraulic properties. Therefore, these surfaces represent additional sinks and sources of momentum, heat and moisture affecting the mechanical, thermodynamical, and hydrological properties of local atmosphere and have specific impact on the meteorological conditions, which is a well-known phenomenon since the 1980s (Oke, 1982, 1987; Godowitch et al., 1985; Eliasson and Holmer, 1990; Haeger-Eugensson and Holmer, 1999).

One of the most comprehensively studied aspects of the meteorological impact of urban surfaces is the Urban Heat Island (UHI) phenomenon which represents an excess warmth of urbanized areas with respect to their non-urbanized (rural) vicinity. UHI forms as a result of modified energy budget due to the canyon-like geometry of the canopy layer and the specific thermal parameters of the artificial surfaces (Oke, 1982). Due to their decreased albedo, urban surfaces store more heat compared to rural areas and after sunset this heat is released with a reduced intensity because of the decreased sky-view factor (Grimmond and Oke, 1995) making UHI typical for night-time, although it is detectable during daytime as well. Some studies performing site measurement in and around cities revealed the so called Urban Cool Island (UCI) effect as well: during the morning hours the enhanced shadowing within urban surfaces delays the heating and causes lower temperatures than over the rural surfaces (Basara et al., 2008; Gaffin et al., 2008).

Urban surfaces have further impact on other meteorological parameters as well: Richards and Oke (2002) and Richards (2004) studied the changes of surface humidity, while Grimmond and Oke (2002), Roth (2000) or Kastner-Klein et al. (2001) focused on the impact on roughness and turbulence. Many studies dealt with the structure of the urban boundary layer including the impact on the height of the planetary boundary layer (ZPBL) (Piringer, 2001; Cleugh and Grimmond, 2001; Martilli, 2002; Angevine et al., 2003; Nair et al., 2004) and wind speeds (Hou et al., 2013). Urbanization-triggered

ACPD
14, 18541–18589, 2014

changes in precipitation and hydrological processes got as well into the attention of research (Dettwiller and Changon, 1976; Shepherd et al., 2002; Rozoff et al., 2003). There is evidence that the urban environment with its higher air pollution is responsible for enhanced lightning (Farias et al., 2009; Coquillat et al., 2013). Schaldach and Alcamo (2007) showed significant influence on the carbon balance as well and, finally, the urban-meteorology interaction may significantly influence air-quality (Rigby and Toumi, 2008; Ryu et al., 2013a, b). However, most of the influences listed here have to be viewed in a common UHI-related framework as they are all physically connected within this phenomenon, bringing higher street level temperatures and having a direct impact on the human health (Reid et al., 2009) and, in general, on the comfort of living.

Numerous studies aimed to find observational (surface measurements, reanalysis or satellite based) evidence for the UHI at different part of the Earth in the past (e.g. Eliasson and Holmer, 1990; Basara et al., 2008; Svoma and Brazel, 2010; Yang et al., 2011; Zhou and Reng, 2011; Giannaros and Melas, 2012; Pichierri et al., 2012). To provide a reliable, numerical modeling based perspective of the UHI phenomenon, and of other related impacts (e.g. on wind speed/direction, precipitation, ZPBL), the complex nature of the mechanical, thermodynamical and radiative processes have to be realistically represented in models. Current operational numerical weather prediction models as well as regional climate models still fail to capture properly the impact of local urban features on the mesoscale meteorology and climate, despite of their increasing resolution. Therefore the inclusion of urban-canopy-models (UCM), which are specially designed to parameterize the processes specific to the urban environment that are not resolvable at the model's scale, is necessary (Baklanov et al., 2008; Lee and Park, 2008; Oleson et al., 2008; Chen et al., 2011).

Along with the development of UCMs, many modeling studies were carried out to describe UHI and other aspect of the urban-atmosphere interaction. Most of the studies focused on a particular city with minor interest in the impact on regional scale further from the urban area itself. Examples of such recent modeling studies include Klaić et al. (2002) for Zagreb, Croatia; Flagg and Taylor (2011) for Detroit-Windsor, USA; Gi-

ACPD
14, 18541–18589, 2014

Title Page
Abstract Introduction
Conclusions References
Tables Figures
◀ ▶
Back Close
Full Screen / Esc
Printer-friendly Version
Interactive Discussion

annaros et al. (2013) for Athens, Greece; Wouters et al. (2013) for Paris, France; Miao et al. (2009) and Hou et al. (2013) for Beijing area, China. These studies conducted experiments for time periods of several days during selected weather episodes only. Furthermore, as mentioned earlier, they focused on the scales of at most a few tens of kilometers around a particular city. Recently, Zhang et al. (2009), Wang et al. (2012) and Feng et al. (2013) examined the impact of urban land-surfaces on the regional climate but with focus on eastern Asia. Over Europe, Struzewska and Kaminski (2012) examined the regional impact of urban surfaces on the forecast of local and regional meteorological conditions and selected pollutants. However, they were not interested in the long-term impacts and performed simulations of only a few tens of hours for three selected episodes. Block et al. (2004) carried out experiments on regional scale over central Europe as well, but they were interested in the impact of the anthropocentric heat release (AHR) only, without any attention to other aspects of urban-climate interactions (e.g. radiation induced UHI phenomenon).

The present study is among the first that aim to examine the regional and long-term impact of all urban surfaces on the regional climate of central Europe. To achieve this goal, the regional climate model RegCM4.2 was coupled with the Single-layer Urban Canopy Model (SLUCM) that accounts for the most relevant processes specific to the urban environment including the AHR. The climate impact of urbanization for day and night time conditions is examined separately, for winter and summer months. The results are evaluated against surface measurements as well. A few sensitivity experiments are carried out to examine the results based on the setting of the key parameters of the SLUCM and on different resolutions of the surface model. Finally, we show how a particular city (Prague) influences the region by disregarding all urban surfaces except those within this city.

2 Tools and experimental set-up

2.1 The regional climate model RegCM4.2

The regional climate model used in this study is the model RegCM version 4.2 (hereafter referred to as RegCM4.2), a 3-D mesoscale model developed at The International Centre for Theoretical Physics (ICTP). In terms of physical parameterizations RegCM4.2 is similar to RegCM3 (Pal et al., 2007). Major changes in the model from version 3 to versions 4.x include the following: the inclusion of the Community Land Surface Model v3.5 (CLM3.5; Tawfik and Steiner, 2011) as an optional land surface parametrization, a new optional parametrizations for diurnal SST variations, and a major restructuring (modularization) of the code base. RegCM4.2 and its evolution from RegCM3 is described in full by Giorgi et al. (2012). Its dynamical core is based on the hydrostatic version of the NCAR-PSU Mesoscale Model version 5 (MM5) (Grell et al., 1994). The radiation is solved using the Community Climate Model version 3 (CCM3) parameterization (Kiehl et al., 1996). The large-scale precipitation and cloud processes are calculated following Pal et al. (2000) and the convection is parameterized (in our case) with the Grell scheme (Grell, 1993) using the Fritsch and Chappell (1980) closure assumption.

RegCM4.2 includes two land-surface models: Biosphere–Atmosphere Transfer Scheme (BATS) originally developed by Dickinson et al. (1993) and the CLM3.5 model (Oleson et al., 2008). An improvement of the BATS scheme is the sub-grid land surface configuration by which each model grid point is divided into a regular sub-grid, and land surface processes are calculated at each sub-grid point taking into account the local landuse and topography (Giorgi et al., 2003).

To describe urbanized surfaces, two new land use types were added to BATS with the introduction of RegCM version 4.0 and higher. These new landuse types alter the values of albedo, roughness length, soil characteristics, maximum vegetation cover in order to account for the modified surface energy balance (heat and momentum), evapotranspiration and runoff specific to urbanized surfaces (parameters are taken from

ACPD
14, 18541–18589, 2014

Kueppers et al., 2008). This represents a bulk parameterization of zero-order effects of urban and suburban landuse types, which however ignores the 3-D character of the processes that occur in urban environment (e.g. in street-canyons). Therefore, we implemented a more sophisticated treatment of the meteorological processes that occur in connection with urban surfaces. Chen et al. (2011) provided an overview of the urban parameterizations that are implemented in the Weather Research and Forecasting model (WRF; Skamarock et al., 2008). For our study, the Single-Layer Urban Canopy Model (SLUCM) is used. It is less complex compared to the multi-layer urban canopy models (MLUCM) and therefore computationally less demanding in long term climate model simulations. On the other hand, it accounts for the 3-D meteorological processes occurring in the cities' environment such as trapping the radiation within the street-canyon, shadowing due to buildings. The following section gives a more detailed description of SLUCM.

2.2 The Single-layer Urban Canopy Model

The Single-layer Urban Canopy Model was developed by Kusaka et al. (2001) and Kusaka and Kimura (2004). It represents the geometry of cities assuming infinitely-long street canyons, where it considers shadowing, reflections, and trapping of radiation and prescribes an exponential wind profile (Fig. 1 for a schematic representation of SLUCM). The model calculates the surface skin temperatures of the roof, wall, and road (determined from the surface energy budget) and temperature profiles within roof, wall, and road layers (determined from the thermal conduction equation) as prognostic variables. Surface-sensible heat fluxes from each surface are calculated using Monin–Obukhov similarity theory and the Jurges formula, which is widely used in the field of architecture (e.g., Tanaka et al., 1993). SLUCM calculates canyon drag coefficient and friction velocity using a similarity stability function for momentum. For a detailed description of the SLUCM, please refer to Kusaka et al. (2001).

The implementation of SLUCM into RegCM4.2 follows the way of its coupling to the WRF model (Chen et al., 2011). SLUCM is coupled to the RegCM4.2 within the BATS surface model, eventually using the BATS's subgrid treatment (SUBBATS). Whenever BATS finds a subgridbox covered by urban surface in the subgrid landuse file, it calls SLUCM routines. The total sensible heat flux from roofs, walls, roads, and the urban canyons is then passed to the RegCM4.2's BATS model. The total momentum flux is passed back in a similar way. BATS then calculates the overall flux for the model grid box by aggregating the fluxes from non-urban and urban surfaces provided by SLUCM. Similarly, the total friction velocity is aggregated from urban and non-urban surfaces and passed to RegCM4.2 boundary-layer scheme. The anthropogenic heat release (AHR) and its diurnal variation are considered by adding them to the sensible heat flux from the urban canopy layer.

2.3 Model configuration and experiments performed

Number of experiments are performed using the RegCM4.2/SLUCM model over 10 km × 10 km resolution domain of 158 × 118 gridpoints covering central Europe. The initial and lateral boundary conditions for RegCM4.2 were taken from the ERA Interim data (Simmons et al., 2007). The BATS was configured with a 2 km × 2 km subgrid set-up, which provides the opportunity to resolve and to describe medium and large continuous urban surfaces (cities) over the targeted area. A further increase of the subgrid division would be definitely beneficial, but it comes with a significant reduction of model speed.

Land use information was compiled using Corine2006 (EEA, 2012) dataset and where it does not provide information (e.g. western Ukraine, Belarus), we used the GLC (2000) database. Two land use categories, urban and sub-urban, are defined. Both land use types are characterized by specific urban geometry parameters (Table 1). Figure 2 presents the gridboxes where urban land-surface category was extracted from the land use data mentioned before (they are usually of sub-urban type and urban land use type is limited to center of the larger cities). The comparison of the 10 km and 2 km spatial grid (left vs. right) clearly shows the need for higher resolution in order to resolve the

Discussion Paper | Discussion Paper | Discussion Paper | Discussion Paper |

ACPD

14, 18541–18589, 2014

fine details of the urbanized surfaces: at coarse resolution, smaller cities cannot be resolved.

The urban canopy parameters used in the SLUCM are the ones used in the WRF implementation of SLUCM (see Chen et al., 2011) modified to better describe the urban environment in cities in central Europe. Building heights were increased and are similar to those used for Polish cities by Struzewska and Kaminski (2012). Similar values were used by Martilli (2002) who focused on European cities as well. The road/street widths are also more suited to the targeted region and follow the values of Martilli (2002) or Ratti et al. (2001). The values for the AHR represent the annual average while the model internally calculates the monthly variation (the yearly amplitude is about 70 % to 130 % of the annual average value for July to January, respectively). They follow the case of a Polish city (Kłysik, 1995) but are also in line with the measurements from the city of Toulouse, France (Pigeon et al., 2007), with the consideration that the central European climate during winter is colder, bringing higher heating and larger heat release. Other parameters of the urban canopy in SLUCM are unchanged from the WRF implementation. It has to be noted that these values are rough estimates and try to describe all the urban (and suburban) surfaces within the domain. However, there are large differences between cities, and even within our 2 km × 2 km subgrid-box, these values can vary substantially. Because of this, a possible uncertainty is brought into the results. To assess its magnitude, a sensitivity test to the key urban parameters was included in this study (Sect. 3.3).

Table 2 summarizes the experiments performed using the RegCM4.2 extended with the SLUCM. The NOURBAN and SLUCM experiments, representing the runs without considering urban surfaces parameterization and with the SLUCM urban canopy treatment, were run for a 5 year period between 2005–2009. The impact of urban surfaces on climate was then evaluated as the difference between SLUCM and NOURBAN for the selected meteorological fields.

To analyze the sensitivity of the results to the key urban parameters, four additional simulations were performed where we modified the building height, street width, roof

ACPD
14, 18541–18589, 2014

albedo and AHR (Table 2). These simulations were performed for a one year period (2005) and are denoted as SEN1–4.

In the noSUBBATS experiment, we examined how the results are modified if the surface model resolution equals to the dynamical resolution (i.e. 10 km). As a reference simulation, a similar experiment is performed without SUBBATS and without any urban treatment (denoted noSUBBATS/NOURBAN). Finally, to see the extent of the urban surfaces' influence on remote areas, we performed an experiment where only Prague was treated as urban surface. Here, Prague is defined as a squared region of 50 km × 50 km area centered on the city's midpoint.

We run RegCM4.2 for year 2004 without SLUCM as a spin-up time, and all the experiments are restarted from this run.

3 Results

3.1 Spatial distribution of the impact of urban surfaces

This section presents the spatial (horizontal and vertical) distribution of the meteorological impacts of urbanized surfaces. To evaluate their seasonal dependence, we present the winter (DJF; December–February) and summer (JJA; June–August) impact separately. Furthermore, as the meteorological regime in urban environment differs between day and night-time, we will discuss separately the day and night impacts as well. Shaded areas in all "spatial" figures represent statistically significant differences at the 95 % level according to the *t* test.

Figure 3 presents the day (upper panels) and night-time (bottom panels) impacts of urban surfaces on the 2 m air temperature averaged over winter (left) and summer (right). In general, the impact is highest over highly urbanized areas indicating a well pronounced UHI effect. The location of cities such as Berlin, Prague, Vienna, Budapest, Munich or Warsaw is well recognized through the UHI effect. In winter, the impact is generally lower, reaching values up to 0.4 K over day-time for many cities. However, the

ACPD
14, 18541–18589, 2014

impact is statistically significant even over rural regions far from larger cities with up to 0.05 K temperature increase. During night, the impact is very small and rather noisy, though there is an indication for a slight temperature decrease over cities up to −0.1 K (over Berlin, Prague, Vienna, Budapest and others).

A much stronger impact is modeled during summer. During the day, temperature is increased almost everywhere over the domain, with a peak over the cities less pronounced than during night-time. The impact exceeds 0.4 K over large part of the domain far from urbanized centers and is highest over Budapest (0.7 K) and Milan (1.0 K). As expected, the most pronounced impact is modeled during the summer night-time when the UHI phenomenon is considered to be the strongest. Over many cities, the temperature increase exceeds 1.5 K (Berlin, Prague, Vienna, Budapest, Munich, Milan, etc.), and is also substantial over rural areas, reaching 0.2 K.

The changes in the height of the planetary boundary layer (ZPBL) are presented in Fig. 4. The daytime impacts are usually more prominent, indicating an increase up to 50 m in winter and up to 200 m in summer months. In winter, the statistically significant changes are usually limited to cities, while in summer, large rural areas are also marked with significant ZPBL increase (up to 50 m over most of the domain). During winter night-time, just a limited number of locations exhibit a significant change, with up to −20 m decrease. In summer, large areas encounter ZPBL increase due to urbanized surfaces (up to 100 m), not limited to just cities. During night-time, the impact of cities is much smaller and is characterized by an increase of ZPBL (up to 50 m). However, over rural areas, a statistically significant decrease is modeled (up to −20 m).

The impact on 10 m wind velocity (Fig. 5) depends largely on whether we consider winter or summer conditions and day or night. In winter day time, urban effects can result in both small increase (usually in the vicinity of the cities) and small decrease of wind speed (located over cities). A more uniform picture is provided for the night-time changes in winter: there is an evident wind speed reduction especially over the cities up to $-0.6\,\mathrm{m\,s^{-1}}$. The decrease over rural areas is small ($-0.1\,\mathrm{m\,s^{-1}}$) and usually statistically insignificant. The impact of cities on wind velocity in summer is characterized, during day-time, by a decrease just over the cities (up to $-0.2\,\mathrm{m\,s^{-1}}$), with a small but statistically significant increase just around the cities (up to $0.2\,\mathrm{m\,s^{-1}}$). During night-time, urban surfaces seem to increase the wind speed up to $0.3\,\mathrm{m\,s^{-1}}$, although this is not evident for all major urban centers throughout central Europe, but rather limited to cities over the western part of the domain.

The impact of urbanized surfaces manifests in a clear evaporation decrease (Fig. 6), mostly over the most populated urban centers. The impact is smallest during night-time in winter (up to $-0.2\,\mathrm{kg\,m^{-2}\,day^{-1}}$), while during summer it reaches $-1\,\mathrm{kg\,m^{-2}\,day^{-1}}$. Similar values are typical during day-time in winter over cities. Finally, the most intense evaporation decrease due to urban surfaces is encountered during summer day-time, as much as $-5\,\mathrm{kg\,m^{-2}\,day^{-1}}$ over many cities and smaller urbanized areas over the domain.

Decrease of evaporation comes along with reduced specific humidity that can be well seen in Fig. 7 (presented for 2 m). The value of this decrease goes in line with the magnitude of evaporation reduction and is smallest during winter night-time (up to $-0.2\,\mathrm{g\,kg^{-1}}$). The winter decrease during day-time is larger, up to $-0.4\,\mathrm{g\,kg^{-1}}$ and is recognizable over number of cities (Budapest, Vienna, Prague, Munich, Berlin etc.). A much larger specific humidity decrease due to urbanized surfaces is modeled during summer, especially for day-time conditions (in accordance with the impact on evaporation) when the decrease can exceed $-1\,\mathrm{g\,kg^{-1}}$ and it is not limited to larger central European cities only (it affects almost the entire domain for both day and night).

The introduction of urban surfaces has impact on the precipitation rate as well in our simulations (Fig. 8). However, the effect is statistically significant only during summer day-time in connection with the decreased evaporation, when it is characterized with large decrease over cities exceeding $-2\,\mathrm{mm\,day^{-1}}$, mostly over Budapest, Katowice, Warsaw, Vienna, Prague, Munich and the Ruhr region in Germany. The precipitation changes over areas without dominant urban surfaces are usually statistically insignificant.

ACPD
14, 18541–18589, 2014

Urban land-surface impact on climate

P. Huszar et al.

Apart from the urban induced changes to the horizontal distribution of meteorological fields, perturbations to the vertical structure of temperature are presented here. Figure 9 illustrates the temperature vertical cross-section along the 50° N latitude which crosses several urbanized areas. A statistically significant warming is indicated up to about 1.7 km in summer, i.e. approximately in the planetary boundary layer (PBL). The warming is most intense just above the surface, but remains above 0.2 K almost across the entire PBL depth during both day and night. The warming due to urban surfaces spreads to lower elevations (300 m) in winter, due to reduced vertical mixing, and is less significant during night. Above the boundary layer in summer (between altitudes 1.7 km and 10 km), statistically significant cooling is modeled, especially during daytime (up to −0.1 K). Finally there is an indication of warming above approximately 10 km (up to 0.05 K), but mostly statistically insignificant. In winter, no statistically significant impact is modeled above the PBL.

3.2 Monthly and daily temperature profiles and comparison with observations

This section presents the impact of urbanized surfaces on the monthly and hourly temperature variations over selected cities in central Europe. Figure 10 shows the monthly 2 m temperatures averaged over years 2005–2009 from both NOURBAN and SLUCM simulations. We also included the corresponding series from the E-OBS gridded observational dataset (Haylock et al., 2008) for comparison. A systematic underestimation of temperatures is revealed, especially during late autumn and early spring (up to −4 K over Berlin). The negative model bias is usually the smallest in August and September. Regarding the impact of urban surface on climate, the SLUCM is slightly warmer than NOURBAN in summer (by about 1 K). In winter, the difference is negligible. This corresponds to the spatial differences seen in Fig. 3. Moreover, the introduction of SLUCM for urban surface treatment clearly reduces the summer model bias: especially over Munich and Budapest the monthly values become very similar to the observations. In case of Vienna, the model even becomes slightly warmer than the measurements.

ACPD
14, 18541–18589, 2014

The 2005–2009 average hourly variation of 2 m temperatures for selected cities is presented in Fig. 11. To obtain information about the magnitude of the UHI effect, we plotted the average temperature from the vicinity of the cities (defined as approximately a 10 km wide belt 20 km from the city centers) taken from the SLUCM experiment. In our simulations, the UHI develops during noon hours and reaches maximum around 10 p.m. to midnight local time at about 0.5 K on annual average. The UHI diminishes around 6 a.m. and is practically zero during morning till noon. It is interesting to see that the city temperatures for configuration disregarding the urban surfaces (NOURBAN, blue line) are lower than the temperatures accounting for urban effect in the vicinity of cities during the maximum UHI development (SLUCM, orange line), by up to 0.1 K on annual average. This is consistent with our spatial results, which showed that the impact of urban surfaces is not limited to the air column over large cities, but is spread over remote areas as well, as seen in Fig. 3.

For more detailed analysis, we used hourly station data from three locations in Prague to compare the observed hourly temperature variations and the modeled summer UHI. One station lies in the inner center of Prague, where the maximum UHI is expected, while two are located in the vicinity of the city center (about 10–15 km far). The results are plotted in Fig. 12. Solid lines stand for the city center model (NOURBAN-blue, SLUCM-pink) and station (orange) data. The dashed and dash-dotted lines correspond to the two stations in Prague's vicinity. As seen already for the monthly data (Fig. 10), there is a negative model bias present throughout the day. When not considering urban surfaces (i.e. the NOURBAN experiment), this bias reaches, during late evening hours, −3 K in city center and around −2 K for the stations in the city's vicinity. When the SLUCM surface model is turned on, an evident model bias reduction is seen during afternoon and evening hours in the city center, i.e. when the UHI achieves its peak. The UHI presence is furthermore indicated by lower temperatures in the city vicinity in both the SLUCM experiment (by almost 0.5 K) and in the measurements (up to 1 K). When we do not consider urban surfaces (NOURBAN experiment, blue line),

ACPD
14, 18541–18589, 2014

the hourly temperature profile is almost the same for the city center and for the two stations in the city vicinity as no urban heat island effect is modeled.

3.3 Sensitivity tests

The urban-canopy model can be configured with a whole range of parameters describing the geometry and the thermomechanical properties of the surfaces typical for urban environment (Table 1). These parameters are set globally without any spatial variation within the domain. Furthermore, for a given gridbox (2 km × 2 km for our subgrid treatment of surface processes), these parameters may, in general, vary from street to street, from building to building. Finally, even choosing these parameters to match the average conditions in urban canopy for a given domain (region) is a challenging task.

Considering the above mentioned, there is a certain degree of uncertainty of the results originating in the estimation of the SLUCM parameters. To evaluate this uncertainty, an additional set of simulations is performed for year 2005 with modified urban canopy parameters. We chose to modify the street width (50 % reduction), building height (50 % reduction), roof albedo (doubled value) and anthropogenic heat release (50 % reduction) corresponding to sensitivity experiments SEN1, SEN2, SEN3 and SEN4, respectively. The first two parameters are of key importance in describing the city's geometry, the third parameter is important in urban mitigation strategies for reducing the UHI. The fourth one is marked with high uncertainty as well, as very few estimations or measurements exist on AHR.

We evaluated the change of spatial distribution of selected meteorological parameters after introducing the modifications of the urban parameters as the difference between the corresponding SENx experiment and SLUCM experiment. We focused on the summer night-time average change when the impacts are large, and in case of the SEN3 sensitivity experiment (reduced albedo) we show the average summer daytime change, as albedo is relevant for the reflected solar radiation.

Figure 13 presents impact on near surface temperature. When reducing building height by 50 %, significant temperature reduction occurs up to −0.4 K over most of the large urbanized areas (cities such Budapest, Vienna, Prague, Berlin, Munich or Warsaw), which corresponds to a 30 % reduction of the absolute impact on temperature (Fig. 3). The reduction of street width by 50 % usually increases summer night-time temperatures up to 0.1–0.2 K, as seen especially over Berlin, Prague, Munich, Vienna. This means an intensification of the UHI phenomenon by about 20 %. Lower roof albedo reflects more solar radiation and this also affects the near surface temperatures during day. Over many cities and even over larger areas around cities, the temperature reduction reaches −0.1 to −0.2 K, which significantly reduces the absolute impact of urban surfaces on temperature seen in Fig. 3. Finally, the AHR reduction reduces also the night time temperatures by up to −0.2 K not only over cities but over areas far from large urbanized centers.

The effects on the PBL height (ZPBL) change within the sensitivity tests are plotted in Fig. 14. The impact on ZPBL is spatially noisier than for the temperature. For the 50 % building height reduction, there is an indication of statistically significant ZPBL decrease of up to −20 m over cities (especially Berlin, Vienna and Warsaw). For the 50 % street width reduction, the ZPBL change pattern is even noisier, without clear impact (slight increase for a few cities, but decrease for others). A more pronounced impact is modeled for the increased roof albedo, when due to enhanced reflection and to lower surface temperatures the PBL stabilizes, decreasing its height. This reduction reaches −30 m over large areas, especially around cities. Finally, when decreasing the AHR, the ZPBL is affected only slightly, with a decrease typically up to −20 m.

For other meteorological parameters, we do not show the spatial results of the sensitivity tests, only the changes for five selected cities. For completeness, we include the near surface temperature and ZPBL as well. The results are presented for both day and night in Table 3, where bold numbers mark statistically significant differences. The table indicates that, as already seen in Fig. 13, reducing building height causes temperature decrease, especially during night (from −0.03 to −0.1 K) while reduced street width results in increased night-time temperatures (0.01 to 0.1 K). The increased roof albedo reduces the day-time temperatures about −0.1 K over cities in central Europe.

Finally, reduced AHR causes temperature decrease during both day and night-time in cities up to −0.1 K. The ZPBL over cities decreases for reduced building height, increased albedo and reduced AHR, but a slight increase is modeled (especially during night-time) when decreasing street width.

The wind speed at 10 m usually increases (up to 0.3 m s^{-1}) when reducing building height, especially during daytime. It further increases over each city during both night and daytime when reducing street width. The reduced roof albedo causes a slight decrease of wind speed which, however, is not statistically significant in most cases. The same is true for the impact of AHR reduction on the wind speed, although the numbers indicate slight decrease.

The 2 m specific humidity (q2m) tends to increase when lowering building heights and to decrease when reducing street width. Decrease occurs over cities as well when roof albedo is raised (especially over Budapest). Finally, with reduced AHR, q2m shows both increase and decrease, but usually of very small magnitude.

The sensitivity runs show a very small effect on total precipitation. When reducing building heights, the precipitation decreases significantly only over Budapest during daytime (−0.4 mm day^{-1}). Over the same city, the reduced street width has significant impact on precipitation, with decrease during daytime but increase during night. Reducing roof albedo leads to significant decrease of precipitation only over Prague and Budapest, over other cities the changes are ambiguous. Finally, reduced AHR leads to a statistically significant decrease of daytime precipitation only over Vienna and Berlin (up to −1 mm day^{-1}).

It is also of interest how the results are influenced by the application of the subgrid surface treatment using the RegCM4.2 SUBBATS feature (at 2 km × 2 km resolution in our case). Figure 15 shows the mean 2005–2009 summer temperature change for day and night evaluated without using SUBBATS. The daytime impact on near surface temperature is relatively smooth and large urban centres are difficult to identify. Maximum impact exceeds 0.2 K, but can reach 1 K in Italy. During night, the urban centres become well visible with usually more than 1 K impact (often more than 1.5 K, i.e. the

ACPD
14, 18541–18589, 2014

Urban land-surface impact on climate

P. Huszar et al.

impact is large over gridboxes with urban landuse category (Fig. 2, left), but is significant even over gridboxes without urban landuse category, often exceeding 0.1 K).

Figure 16 presents the impact of urban surfaces corresponding only to Prague on the near surface temperature (incl. the SUBBATS treatment). The statistically significant temperature impact is limited to a small region (up to 150 km in diameter) around Prague for both day and night. The maximum impact corresponds to the Prague city centre and reaches 0.4 and 1.0 K for day and night, respectively, which is, for night-time, slightly less compared to the case when all the urban surfaces are considered (Fig. 3).

4 Discussion and conclusions

We evaluated the regional impact of urban surfaces on the meteorological conditions over central Europe using the regional climate model RegCM4.2 extended with a single-layer urban canopy model. We focused on the long term effects performing 5 year simulations.

In terms of temperature, the largest impacts are modeled during summer night-time with up to 1.5 K higher temperatures than without considering urban surfaces. This is consistent with the maximum UHI development during evening and night hours seen in previous studies for European cities (Eliasson and Holmer, 1990 for Goteborg; Pichierri et al., 2012 for Milan; Giannaros and Melas, 2012 for Thessaloniki; Giannaros et al., 2013 for Athens) or for US cities (e.g. Oleson et al., 2008). In winter, the impact is significant mainly during daytime (seen similarly in Struzewska and Kaminski, 2012), which is probably due to governing role of AHR being stronger during the day. Feng et al. (2012) found AHR the most important factor influencing the urban impact on winter temperatures.

It is also found that the impact of urban surfaces on temperature spreads, especially during summer, across the whole PBL, which is caused by enhanced vertical mixing in summer. The modeled decrease of temperature over the PBL can be explained by the increased vertical lapse rate due to higher PBL temperature, resulting in enhanced convection, as discussed by Collier (2006).

In our simulations, the PBL height increases in both winter and summer daytime, and summer night-time, but decrease is modeled over cities in winter night-time. The day-time increase is explained by enhanced turbulent mixing due to the urban morphology as found by many (Martilli, 2002; Angevine et al., 2003; Rotach et al., 2005; Collier, 2006). The summer night-time PBL increase is limited over cities and can be the result of warmer air in the nocturnal PBL due to UHI. In winter night-time, a slight PBL height reduction is modeled that is attributable to decreased wind speeds (see below), thus decreased mixing.

The wind speed changes in summer daytime are characterized with a slight decrease over cities. Similar decreases were found by Klaić et al. (2002) or Hou et al. (2013). The increase in wind speed during night-time can be related to urban-breeze circulation, when, in the presence of thermally induced horizontal pressure gradient, convergent motions towards the city form (Hidalgo et al., 2010).

The impact of urban surfaces on evaporation is evident for both seasons, but stronger in summer due to higher temperatures. It is a direct result of higher runoff in cities, related to reduced capability of urban structures to accumulate water that would be later available for evaporation. The reduced evaporation then causes lower specific humidity, especially during summer, when the largest changes are modeled in term of evaporation.

Our results suggest almost no impact of urbanization on winter precipitation and that of summer night-time. However, a statistically significant decrease of rainfall is modeled in summer during day. There has been evidence in other studies (e.g. Kaufmann et al., 2007) that within urban environment, the rain formation is suppressed, due to decreased availability of moisture. On the other hand, over cities in summer, convection is enhanced, which however brings more precipitation a few tens of kilometers downwind from cities, as modeled or observed by many authors (e.g. Shepherd et al., 2002; Rozoff et al., 2003). This enhancement is seen in our results, if we omit the significance

ACPD
14, 18541–18589, 2014

test. Indeed, we simulated a slight increase in precipitation further from cities but these results are not statistically significant in our simulations.

The comparison of monthly temperature data over cities with measurements reveals a negative model bias throughout the year, with maximum discrepancy in early spring. It is probably due to overestimation of cloudiness in our simulations. However, applying the SLUCM urban canopy treatment, the negative bias in summer is reduced or, in some cases, vanishes entirely. Improvement in model performance is evident from the comparison of diurnal temperature variation with observed temperatures as well. The negative model bias is significantly reduced during afternoon and evening hours when the urban meteorological effects are most prominent.

It is important to emphasize that, regarding the temperature, the impact of urban surfaces we modeled is not identical to the UHI magnitude, as the UHI is defined as the temperature difference between the city center and its urban effect-free vicinity. We demonstrated in our simulations that the cities impact temperatures over rural areas as well. Hence, the reference state corresponding to the absence of urban surfaces (the NOURBAN experiment) is colder than the reference for the UHI magnitude calculation at a particular city. This was well seen in the plots showing the hourly temperature variation over selected cities where the temperatures in the city's vicinity are higher than if there were no cities at all. Then, the annual mean UHI magnitude is 0.5–1 K. Unger et al. (2011) provide information on the annual mean UHI from a middle sized central European city of Novi Sad in Serbia and they find UHI up to 4 K. However, this value is representative of the very center of the city of a few square kilometers, while in our simulations we averaged the temperature from a 10 km × 10 km gridbox. If the UHI values from the aforementioned study are averaged over such an area around the city center, the values become 1–2 K, which is closer to our results. The same is true for Bottyan and Unger (2003) who provide mean maximum UHI intensity of 2.1 K and 3.1 K for the Hungarian city of Szeged during heating and non-heating season, respectively. Pongrácz et al. (2010) report on the UHI intensity in central European cities, based on satellite data, found the 2001–2003 mean night-time UHI to be around 2 K. They

ACPD
14, 18541–18589, 2014

defined the city as a 15 km radius circle around the center and a 15–25 km belt around represented the rural areas for determining the UHI. This corresponds well to our definition and suggests an underestimation of UHI in our simulations. A more pronounced UHI was simulated by Fallmann et al. (2013) as well for Stuttgart (around 2.5 K, compared to our value of about 0.7 K). They, however, used a much finer resolution of 1 km × 1 km and the city averaged UHI intensity (1.3 K), which is a more comparable quantity with our values, is again closer to our result. It have to be also added that their experiments were carried out for a exceptionally warm period of 11 to 18 August during the 2003 heat wave, while we averaged over summers from 5 years that include also cloudy days when the sunshine and consequently the UHI is suppressed.

The sensitivity analysis for the summer meteorological conditions showed a rather limited dependence on the model setup of the geometric and radiative characteristics of the urban environment. Specifically, the temperature responses to significant changes of geometry parameters such as street width or building height are of the order 0.01 K (up to 0.1 K in a few cases). The same is true for the AHR. Somewhat stronger temperature response was detected for the building roof albedo value. The changes of the boundary layer height can be as high as a few tens of meters when perturbing the key SLUCM parameters in our simulations, which is closer to the average modeled ZPBL change (Fig. 4) and reveals relatively large sensitivity of ZPBL to urban parameters. Similarly, a substantial dependence of the 10 m wind velocity on the urban geometry parameters is modeled (with changes in the order of 0.1 m s^{-1}), which is comparable to the absolute impact of urban surfaces. The roof albedo and the AHR had a very little impact on the wind speed. The dependence of the impact on the humidity is small, but often statistically significant, especially when reducing the AHR. Finally, precipitation can be impacted largely when changing the SLUCM parameters (up to −1 mm day^{-1} when reducing AHR), but these changes are usually insignificant in a statistical sense. Therefore, we can conclude that the results concerning the impact of urbanized surfaces on the long term meteorological conditions over central Europe are, with respect to the overall uncertainty of parameters settings, quite robust and efforts aiming to set the urban parameters more precisely with the eventuality of using 2-D distribution of these parameters will change the overall picture probably only a little.

Another important conclusion about the impact of urban surfaces on temperature is that in central Europe they are not limited to large cities only, but can be significant over remote areas with rather minor urban development as well. A question arises whether this impact is the result of the presence of more smaller cities, i.e. a few urbanized subgrid boxes in the corresponding 10 km × 10 km gridboxes, or whether urban surfaces have distant influence on non-urbanized areas far from them. Figure 2 (right) shows that at 2 km × 2 km resolution, the domain is densely populated by urban surfaces and, actually, most of the corresponding 10 km × 10 km gridboxes really contain at least a few urban subgrid boxes. These might contribute to the impact on the whole gridbox depending roughly on the percentual urban coverage of the gridbox. Indeed, we saw in Fig. 15 that if using only the 10 km × 10 km resolution, the temperature impact is significantly larger over these gridboxes than elsewhere. On the other hand, there is still a relatively large impact over non-urbanized gridboxes that can reach 0.2 K, and which could be attributed to the remote impact of UHI. However, Fig. 3 shows that for nighttime conditions over areas with minor urbanization, such impact is slightly higher (by 0.05 K). This indicates that these small urban elements (smaller cities, sub-urban and partly urbanized areas) can contribute to the impact. This conclusion could partially affect, at least in the areas with highly populated urbanized areas like in Europe, the of temperature increase under global warming, supposing the rapid development of the urbanization in the region.

The second question relates to the remotness of the urban impact, i.e. how purely rural areas can be influenced by nearby (or even more distant) cities. In Fig. 16, the impact of Prague is apparently limited to the surrounding region of no more than 150 km diameter, elsewhere the impact is statistically insignificant (except a little noise which has not been eliminated using 5 years long simulations and 95 % significance threshold). In conclusion, we can state that over remote areas the modeled temperature impact is a combination of the distant impact of surrounding large urbanized areas and

ACPD
14, 18541–18589, 2014

the local impact of the few small urbanized sub-gridboxes located in the corresponding gridbox. The remote impact is probably caused by the advection of warm air originating from UHI over non-urbanized areas. This is well seen especially during day (in summer), when wind speed is higher, resulting in smooth, almost uniform urban impact on temperature across the domain. Feng et al. (2012) simulated the long term regional impact of urbanization and AHR and found values similar to our study: over most of the eastern China exceeding 1 K for summer average.

A question remains what improvement of the results can be achieved by using a more sophisticated urban canopy model, such as the multilayer BEP (Building Energy Parameterization) model (Martilli et al., 2002). It will certainly better describe the 3-D nature of the heat, moisture and momentum exchange between buildings and street-canyon, impacting the thermodynamic structure of the urban roughness sub-layer and hence the lower part of the urban boundary layer. Although a multi-layer urban canopy model represents an increase of computational demand compared to SLUCM, future work should focus in this direction and apply such models in long term climate simulations in combination with regional climate models, in order to obtain a more accurate picture about the climatic impact of urbanization on regional scale.

The results obtained in this study have implications in atmospheric chemistry as well. As the chemical transformation, transport, diffusion and deposition of chemical species and aerosols are strongly linked to the meteorological (thus climate) conditions, the urban canopy induced changes we calculated here may, in general, have impact on the air quality as well. This was a subject of a few studies focusing on London and Soeul (Rigby and Toumi, 2008; Ryu et al., 2013a, b). A future study we plan, will deal with the potential consequences on the air-quality over central Europe as well.

Acknowledgements. This work has been funded by the Czech Science Foundation (GACR) project No. 13-19733P as well as by the project UHI funded in the framework of EC OP NN (No. 3 CE292P3), the program PRVOUK – Environmental Research of the Charles University in Prague and, partially, by the project UNCE 204020/2013. We further acknowledge the E-OBS dataset from the EU-FP6 project ENSEMBLES (http://ensembles-eu.metoffice.com) and the data providers in the ECA&D project (http://www.ecad.eu).

ACPD
14, 18541–18589, 2014

References

Angevine, W. M., White, A. B., Senff, C. J., Trainer, M., Banta, R. M., and Ayoub, M. A.: Urban-rural contrasts in mixing height and cloudiness over Nashville in 1999, J. Geophys. Res., 108, 4092, doi:10.1029/2001JD001061, 2003. 18543, 18559

Baklanov, A., Korsholm, U., Mahura, A., Petersen, C., and Gross, A.: ENVIRO-HIRLAM: on-line coupled modelling of urban meteorology and air pollution, Adv. Sci. Res., 2, 41–46, doi:10.5194/asr-2-41-2008, 2008. 18544

Basara, J. B., Hall Jr., P. K., Schroeder, A. J., Illston, B. G., and Nemunaitis, K. L.: Diurnal cycle of the Oklahoma City urban heat island, J. Geophys. Res., 113, D20109, doi:10.1029/2008JD010311, 2008. 18543, 18544

Block, A., Keuler, K., and Schaller, E.: Impacts of anthropogenic heat on regional climate patterns, Geophys. Res. Lett., 31, L12211, doi:10.1029/2004GL019852, 2004. 18545

Bottyan, Z. and Unger, J.: A multiple linear statistical model for estimating the mean maximum urban heat island, Theor. Appl. Climatol., 75, 233–243, 2003. 18560

Chen, F., Kusaka, H., Bornstein, R., Ching, J., Grimmond, C. S. B., Grossman-Clarke, S., Loridan, T., Manning, K. W., Martilli, A., Miao, S., Sailor, D., Salamanca, F. P., Taha, H., Tewari, M., Wang, X., Wyszogrodzki, A. A., and Zhang, C.: The integrated WRF/urban modelling system: development, evaluation, and applications to urban environmental problems, Int. J. Climatol., 31, 273–288, 2011. 18544, 18547, 18549, 18574

Cleugh, H. A. and Grimmond, C. S. B.: Modelling regional scale surface energy exchanges and CBL growth in a heterogeneous, urbanrural landscape, Bound.-Lay. Meteorol., 98, 1–31, 2001. 18543

Collier, C. G.: The impact of urban areas on weather, Q. J. Roy. Meteor. Soc., 132, 1–25, 2006. 18559

Coquillat, S., Boussaton, M.-P., Buguet, M., Lambert, D., Ribaud, J.-F., and Berthelot, A.: Lightning ground flash patterns over Paris area between 1992 and 2003: influence of pollution?, Atmos. Res., 122, 77–92, doi:10.1016/j.atmosres.2012.10.032, 2013. 18544

Dettwiller, J. and Changnon, S. A.: Possible urban effects on maximum daily rainfall at Paris, St. Louis and Chicago, J. Appl. Meteorol., 15, 518–519, 1976. 18544

Dickinson, R. E., Henderson-Sellers, A., and Kennedy, P.: Biosphere–atmosphere transfer scheme (BATS) version 1 as coupled to the NCAR community climate model. Tech Rep,

ACPD
14, 18541–18589, 2014

Urban land-surface impact on climate

P. Huszar et al.

National Center for Atmospheric Research Tech Note NCA R.TN-387+STR, NCAR, Boulder, CO, 1993. 18546
EEA: Corine Land Cover 2006 technical guidelines, EEA (European Environment Agency), OPOCE (Office for Official Publications of the European Communities), Copenhagen, 2012. 18548
Eliasson, I. and Holmer, B.: Urban heat island circulation in Goteborg, Sweden, Theor. Appl. Climatol., 42, 187–196, 1990. 18543, 18544, 18558
Fallmann, J., Emeis, S., and Suppan, P.: Mitigation of urban heat stress – a modelling case study for the area of Stuttgart, Die Erde, 144, 202–216 doi:10.12854/erde-144-15, 2013. 18561
Farias, W. R. G., Pinto Jr., O., Naccarato, K. P., and Pinto, I. R. C. A.: Anomalous lightning activity over the Metropolitan Region of São Paulo due to urban effects, Atmos. Res., 91, 485–490, 2009. 18544
Feng, J.-M., Wang, Y.-L., Ma, Z.-G., and Liu, Y.-H.: Simulating the regional impacts of urbanization and anthropogenic heat release on climate across china, J. Climate, 25, 7187–7203, doi:10.1175/JCLI-D-11-00333.1, 2012. 18558, 18563
Feng, J.-M., Wang, Y.-L., and Ma, Z.-G.: Long-term simulation of large-scale urbanization effect on the East Asian monsoon, Clim. Change, 1–13, doi:10.1007/s10584-013-0885-2, 2013. 18545
Flagg, D. D. and Taylor, P. A.: Sensitivity of mesoscale model urban boundary layer meteorology to the scale of urban representation, Atmos. Chem. Phys., 11, 2951–2972, doi:10.5194/acp-11-2951-2011, 2011. 18544
Fritsch, J. M. and Chappell, C. F.: Numerical prediction of convectively driven mesoscale pressure systems, Part I: Convective parameterization, J. Atmos. Sci., 37, 1722–1733, 1980. 18546
Gaffin, S. R., Rosenzweig, C., Khanbilvardi, R., Parshall, L., Mahani, S., Glickman, H., Goldberg, R., Blake, R., Slosberg, R. B., and Hillel, D.: Variations in New York City's urban heat island strength over time and space, Theor. Appl. Climatol., 94, 1–11, doi:10.1007/s00704-007-0368-3, 2008. 18543
Giannaros, T. M. and Melas, D.: Study of the urban heat island in a coastal Mediterranean city: the case study of Thessaloniki, Greece, Atmos. Res., 118, 103–120, doi:10.1016/j.atmosres.2012.06.006, 2012. 18544, 18558

ACPD
14, 18541–18589, 2014

Urban land-surface impact on climate

P. Huszar et al.

Giannaros, T. M., Melas, D., Daglis, I. A., Keramitsoglou, I., and Kourtidis, K.: Numerical study of the urban heat island over Athens (Greece) with the WRF model, Atmos. Environ., 73, 103–111, doi:10.1016/j.atmosenv.2013.02.055, 2013. 18544, 18558

Giorgi, F., Francisco, R., and Pal, J. S.: Effects of a sub-grid scale topography and landuse scheme on surface climate and hydrology. I. Effects of temperature and water vapor disaggregation, J. Hydrometeorol., 4, 317–333, 2003. 18546

Giorgi, F., Coppola, E., Solmon, F., Mariotti, L., Sylla, M., Bi, X., Elguindi, N., Diro, G. T., Nair, V., Giuliani, G., Cozzini, S., Guettler, I., O'Brien, T. A., Tawfi, A. B., Shalaby, A., Zakey, A., Steiner, A., Stordal, F., Sloan, L., and Brankovic, C.: RegCM4: Model description and preliminary tests over multiple CORDEX domains, Clim. Res., 52, 7–29, 2012. 18546

GLC: Global Land Cover 2000 database. European Commission, Joint Research Centre, available at: http://bioval.jrc.ec.europa.eu/products/glc2000/glc2000.php (last access: 14 July 2014), 2000. 18548

Godowitch, J. M., Ching, J. K. S., and Clarke, J. F.: Evolution of the nocturnal inversion layer at an urban and nonurban site, J. Appl. Meteorol. Clim., 24, 791–804, 1985. 18543

Grell, G.: Prognostic evaluation of assumptions used by cumulus parameterizations, Mon. Weather Rev., 121, 764–787, 1993. 18546

Grell, G., Dudhia, J., Stauffer, D. R.: A description of the fifth generation Penn State/NCAR Mesoscale Model (MM5), National Center for Atmospheric Research Tech Note NCAR/TN-398 + STR, NCAR, Boulder, CO, 1994. 18546

Grimmond, C. S. B. and Oke, T. R.: Comparison of heat fluxes from summertime observations in the suburbs of four North American cities. J. Appl. Meteorol., 34, 873–889, 1995. 18543

Grimmond, C. S. B. and Oke, T. R.: Turbulent heat fluxes in urban areas: Observations and a local-scale urban meteorological parameterization scheme (LUMPS), J. Appl. Meteorol., 41, 792–810, 2002. 18543

Haeger-Eugensson, M. and Holmer, B.: Advection caused by the UHIC as a regulating factor on the nocturnal UHI, Int. J. Climatol., 19, 975–988, 1999. 18543

Haylock, M. R., Hofstra, N., Klein Tank, A. M. G., Klok, E. J., Jones, P. D., and New, M.: A European daily high-resolution gridded dataset of surface temperature and precipitation. J. Geophys. Res.-Atmos., 113, D20119, doi:10.1029/2008JD010201, 2008. 18553

Hidalgo, J., Masson, V., and Gimeno, L.: Scaling the Daytime Urban Heat Island and Urban-Breeze Circulation, J. Appl. Meteorol. Clim., 49, 889–901, 2010. 18559

Hou, A., Ni, G., Yang, H., and Lei, Z.: Numerical Analysis on the Contribution of Urbanization to Wind Stilling: an Example over the Greater Beijing Metropolitan Area, J. Appl. Meteorol. Clim., 52, 1105–1115, doi:10.1175/JAMC-D-12-013.1, 2013. 18543, 18545, 18559

Kastner-Klein, P., Fedorovich, E., and Rotach, M. W.: A wind tunnel study of organised and turbulent air motions in urban street canyons, J. Wind Eng. Ind. Aerod., 89, 849–861, 2001. 18543

Kaufmann, R. K., Seto, K. C., Schneider, A., Liu, Z., Zhou, L., and Wang, W.: Climate response to rapid urban growth: evidence of a human-induced precipitation deficit, J. Climate 20, 2299–2306, 2007. 18559

Kiehl, J., Hack, J., Bonan, G., Boville, B., Breigleb, B., Williamson, D., and Rasch, P.: Description of the NCAR Community Climate Model (CCM3). National Center for Atmospheric Research Tech Note NCAR/TN-420+STR, NCAR, Boulder, CO, 1996. 18546

Klaić, Z. B., Nitis, T., Kos, I., and Moussiopoulos, N.: Modification of local winds due to hypothetical urbanization of the Zagreb surroundings, Meteorol. Atmos. Phys., 79, 1–12, 2002. 18544, 18559

Kłysik, K.: Spatial and seasonal distribution of anthropogenic heat emissions in Åodz, Poland, Atmos. Environ., 30, 3397–3404, 1995. 18549

Kueppers, L. M., Snyder, M. A., Sloan, L. C., Cayan, D., Jin, J., Kanamaru, H., Kanamitsu, M., Miller, N. L., Tyree, M., Du, H., and Weare, B.: Seasonal temperature response to land-use change in the western United States, Global Planet. Change, 60, 250–264, 2008. 18547

Kusaka, H., Kondo, H., Kikegawa, Y., and Kimura, F.: A simple singlelayer urban canopy model for atmospheric models: comparison with multi-layer and slab models, Bound.-Lay. Meteorol., 101, 329–358., 2001. 18547

Kusaka, H., and Kimura, F.: Coupling a single-layer urban canopy model with a simple atmospheric model: impact on urban heat island simulation for an idealized case, J. Meteorol. Soc. Jpn., 82, 67–80, 2004. 18547

Lee, S.-H. and Park, S.-U.: A vegetated urban canopy model for meteorological and environmental modelling, Bound.-Lay. Meteorol., 126, 73–102, 2008. 18544

Martilli, A: Numerical study of urban impact on boundary layer structure: sensitivity to wind speed, urban morphology, and rural soil moisture, J. Appl. Meteorol., 41, 1247–1266, 2002. 18543, 18549, 18559

Martilli, A., Clappier, A., and Rotach, M. W.: An urban surface exchange parameterization for mesoscale models, Bound.-Lay. Meteorol., 104, 261–304, 2002. 18563

ACPD
14, 18541–18589, 2014

Urban land-surface impact on climate

P. Huszar et al.

Miao, S., Chen, F., LeMone, A. M., Tewari, M., Li, Q., and Wang, Y., 2009: An observational and modelling study of characteristics of urban heat island and boundary layer structures in Beijing, J. Appl. Meteorol. Clim., 48, 484–501, 2009. 18545

Nair, K. N., Freitas, E. D., Sanchez-Ccoyllo, O. R., Dias, M., Dias, P. L. S., Andrade, M. F., and Massambani, O.: Dynamics of urban boundary layer over Sao Paulo associated with mesoscale processes, Meteorol. Atmos. Phys., 86, 87–98, 2004. 18543

Oke, T. R.: The energetic basis of the urban heat island, Q. J. Roy. Meteor. Soc., 108, 1–24, doi:10.1002/qj.49710845502, 1982. 18543

Oke, T. R.: Boundary Layer Climates, Methuen and Co. Ltd, London, 2nd edn., 1987. 18543

Oleson, K. W., Bonan, J. B., Feddema, J., Vertenstein, M., and Grimmond, C. S. B.: An urban parameterization for a global climate model, Part I: Formulation and evaluation of two cities, J. Appl. Meteorol. Clim., 47, 1038–1060, 2008. 18544, 18546, 18558

Pal, J. S., Small, E. E., and Eltahir, E. A. B.: Simulation of regional-scale water and energy budgets: Representation of subgrid cloud and precipitation processes within RegCM, J. Geophys. Res.-Atmos., 105, 29579–29594, 2000. 18546

Pal, J. S., Giorgi, F., Bi, X., Elguindi, N., Solmon, F., Gao, X., Rauscher, S. A., Francisco, R., Zakey, A., Winter, J., Ashfaq, M., Syed, F. S., Bell, J. L., Diffenbaugh, N. S., Karmacharya, J., Konare, A., Martinez, D., da Rocha, R. P., Sloan, C., and Steiner, A. L.: The ICTP RegCM3 and RegCNET: regional climate modeling for the developing world, B. Am. Meterol. Soc., 88, 1395–1409, 2007. 18546

Pichierri, M., Bonafoni, S., and Biondi, R.: Satellite air temperature estimation for monitoring the canopy layer heat island of Milan, Remote Sens. Environ., 127, 130–138, doi:10.1016/j.rse.2012.08.025, 2012. 18544, 18558

Pigeon, G., Legain, D., Durand, P., and Masson, V.: Anthropogenic heat release in an old European agglomeration (Toulouse, France), Int. J. Climatol., 27, 1969–1981, 2007. 18549

Piringer, M.: Exploring the urban boundary layer by sodar and tethersonde, Phys. Chem. Earth Pt. B., 26, 881–885, 2001. 18543

Pongrácz, R., Bartholy, J., and Dezső, Z.: Application of remotely sensed thermal information to urban climatology of Central European cities, Phys. Chem. Earth, 35, 95–99, doi:10.1016/j.pce.2010.03.004, 2010. 18560

Ratti, C., Di Sabatino, S., Britte, R., Brown, M., Caton, F., and Burian, S.: Analysis of 3-D urban databases with respect to pollution dispersion for a number of European and American cities, Water Air Soil Poll., 2, 459–469, 2001. 18549

ACPD
14, 18541–18589, 2014

Reid, C. E., O'Neill, M. S., Gronlund, C. J., Brines, S. J., Brown, D. G., Diez-Roux, A. V., and Schwartz, J.: Mapping community determinants of heat vulnerability, Environ. Health Persp., 117, 1730–1736, doi:10.1289/ehp.0900683, 2009. 18544

Richards, K.: Observation and simulation of dew in rural and urban environments, Prog. Phys. Geog., 28, 76–94, 2004. 18543

Richards, K., and Oke, T. R.: Validation and results of a scale model of dew deposition in urban environments, Int. J. Climatol., 22, 1915–1933, 2002. 18543

Rigby, M., Toumi, R.: London air pollution climatology: indirect evidence for urban boundary layer height and wind speed enhancement, Atmos. Environ., 42, 4932–4947, doi:10.1016/j.atmosenv.2008.02.031, 2008. 18544, 18563

Rotach, M. W., Richner, H., Vogt, R., Christen, A., Parlow, E., Bernhofer, C., Batchvarova, E., Clappier, A., Roulet, Y.-A., Feddersen, B., Schatzmann, M., Batchvarova, E., Gryning, S.-E., Mayer, H., Martucci, G., Mitev, V., Oke, T. R., Roth, M., Ruffieux, D., Salmond, J. A., Voogt, J. A.: BUBBLE-an urban boundary layer project, Theor. Appl. Climatol., 81, 231–261, 2005. 18559

Roth, M.: Review of atmospheric turbulence over cities, Q. J. Roy. Meteor. Soc., 126, 941–990, 2000. 18543

Rozoff, C. M., Cotton, W. R., and Adegoke, J. O.: Simulation of St. Louis, Missouri, land use impacts on thunderstorms, J. Appl. Meteorol., 42, 716–738, 2003. 18544, 18559

Ryu, Y.-H., Baik, J.-J., Kwak, K.-H., Kim, S., and Moon, N.: Impacts of urban land-surface forcing on ozone air quality in the Seoul metropolitan area, Atmos. Chem. Phys., 13, 2177–2194, doi:10.5194/acp-13-2177-2013, 2013a. 18544, 18563

Ryu, Y.-H., Baik, J.-J., and Lee, S.-H.: Effects of anthropogenic heat on ozone air quality in a megacity, Atmos. Environ., 80, 20–30, doi:10.1016/j.atmosenv.2013.07.053, 2013b. 18544, 18563

Schaldach, R. and Alcamo, J.: Simulating the effects of urbanization, afforestation and cropland abandonment on a regional carbon balance: a case study for Central Germany, Reg. Environ. Change, 7, 137–148, doi:10.1007/s10113-007-0034-4, 2007. 18544

Shepherd, J. M., Pierce, H., and Negri, A. J.: Rainfall modification by major urban areas: observations from spaceborne rain radar on the TRMM satellite, J. Appl. Meteorol., 41, 689–701, 2002. 18544, 18559

ACPD

14, 18541–18589, 2014

Simmons, A., Uppala, S., Dee, D., and Kobayashi, S.: ERA-Interim: New ECMWF Reanalysis Products from 1989 Onwards, Newsletter 110, Winter 2006/07, ECMWF, Reading, 2007. 18548

Skamarock, W. C., Klemp, J. B., Dudhia, J., Gill, D. O., Barker, D. M., Duda, M., Huang, X.-Y., Wang, W., and Powers, J. G.: A Description of the Advanced Research WRF Version 3 NCAR Technical Note, National Center for Atmospheric Research, Boulder CO, USA, doi:10.5065/D68S4MVH, 2008. 18547

Struzewska, J. and Kaminski, J. W.: Impact of urban parameterization on high resolution air quality forecast with the GEM – AQ model, Atmos. Chem. Phys., 12, 10387–10404, doi:10.5194/acp-12-10387-2012, 2012. 18545, 18549

Svoma, B. M. and Brazel, A.: Urban effects on the diurnal temperature cycle in Phoenix, Arizona, Clim. Res., 41, 21–29, 2010. 18544

Tanaka, S., Takeda, H., Adachi, T., and Tsuchiya, T.: Architectural Environmental Engineering, Inoue Co., Ltd., Tokyo, 301 pp., 2013 (in Japanese). 18547

Tawfik, A. B. and Steiner, A. L.: The role of soil ice in land–atmosphere coupling over the United States: a soil moisture precipitation winter feedback mechanism. J. Geophys. Res., 116, D02113, doi:10.1029/2010JD014333, 2011. 18546

Unger, J., Savić, S., and Gál, T.: Modelling of the annual mean urban heat island pattern for planning of representative urban climate station network, Adv. Meteorol., 2011, ID398613, doi:10.1155/2011/398613, 2011. 18560

Yang, X., Hou, Y., and Chen, B.: Observed surface warming induced by urbanization in east China, J. Geophys. Res., 116, D14113, doi:10.1029/2010JD015452, 2011. 18544

Wang, J., Feng, J., Yan, Z., Hu, Y., and Jia, G.: Nested high-resolution modeling of the impact of urbanization on regional climate in three vast urban agglomerations in China, J. Geophys. Res., 117, D21103, doi:10.1029/2012JD018226, 2012. 18545

Wouters, H., De Ridder, K., Demuzere, M., Lauwaet, D., and van Lipzig, N. P. M.: The diurnal evolution of the urban heat island of Paris: a model-based case study during Summer 2006, Atmos. Chem. Phys., 13, 8525–8541, doi:10.5194/acp-13-8525-2013, 2013. 18545

Zhang, H., Gao, X., and Li, Y.: Climate impacts of land-use change in China and its uncertainty in a global model simulation, Clim. Dynam., 32, 473–494, 2009. 18545

Zhou, Y. and Ren, G.: Change in extreme temperature event frequency over mainland China, 1961–2008, Clim. Res., 50, 125–139, 2011. 18544

ACPD
14, 18541–18589, 2014

Table 1. Urban canopy parameters of SLUCM as implemented in RegCM4.2 for the central European region.

Parameter	Unit	Urban	Sub-urban
h (building height)	m	20	15
l_{roof} (roof width)	m	20	15
l_{road} (street width)	m	15	20
AH (anthropogenic heat)	$W\,m^{-2}$	70	30
F_{urb} (urban fraction)	–	0.9	0.7
C_R (heat capacity of the roof)	$J\,m^{-3}\,K^{-1}$	1.0×10^6	1.0×10^6
C_W (heat capacity of the wall)	$J\,m^{-3}\,K^{-1}$	1.0×10^6	1.0×10^6
C_G (heat capacity of the road)	$J\,m^{-3}\,K^{-1}$	1.4×10^6	1.4×10^6
λ_R (thermal conductivity of the roof)	$J\,m^{-1}\,s^{-1}\,K^{-1}$	0.67	0.67
λ_W (thermal conductivity of the wall)	$J\,m^{-1}\,s^{-1}\,K^{-1}$	0.67	0.67
λ_G (thermal conductivity of the road)	$J\,m^{-1}\,s^{-1}\,K^{-1}$	0.40	0.40
α_R (albedo of the roof)	–	0.20	0.20
α_W (albedo of the wall)	–	0.20	0.20
α_G (albedo of the road)	–	0.20	0.20
ε_R (emissivity of the roof)	–	0.90	0.90
ε_W (emissivity of the wall)	–	0.90	0.90
ε_G (emissivity of the road)	–	0.95	0.95
Z_{0R} (roughness length for momentum over roof)	m	0.01	0.01

ACPD
14, 18541–18589, 2014

Table 2. Different experiments performed with the RegCM4.2/SLUCM couple. The sensitivity runs are described in terms of the percentual change of the selected urban parameter with respect to the value listed in Table 1.

Experiment	Urban treatment	Period	SLUCM parameters	SUBBATS	Urban surfaces
NOURBAN	No	2005–2009	–	Yes	–
SLUCM	Yes	2005–2009	Default – see Table 1	Yes	All
SEN1	Yes	2005	50 % building height	Yes	All
SEN2	Yes	2005	50 % road width	Yes	All
SEN3	Yes	2005	200 % roof albedo	Yes	All
SEN4	Yes	2005	50 % AHR	Yes	All
noSUBBATS	Yes	2005–2009	Default – see Table 1	No	All
noSUBBATS/NOURBAN	No	2005–2009	–	No	–
PRAGUE	Yes	2005–2009	Default – see Table 1	Yes	Prague only

ACPD
14, 18541–18589, 2014

Urban land-surface impact on climate

P. Huszar et al.

Table 3. Sensitivity tests: changes in selected meteorological parameters (T_{2m} – 2 m temperature [K], Z_{pbl} – planetary boundary layer height [m], V_{10m} – wind speed at 10 m [m], Q_{2m} – specific humidity at 2 m [g kg^{-1}], P_{tot} – total precipitation rate [mm day^{-1}]) over five cities due to changes in urban canopy parameters of SLUCM for day and night-time in summer 2005. Bold numbers indicate statistically significant differences on the 95 % level.

		Prague		Vienna		Budapest		Munich		Berlin	
		JJA day	JJA night	JJA day	JJA night	JJA day	JJA night	JJA day	JJA night	JJA day	JJA night
SEN1	T_{2m}	−0.02	**−0.03**	−0.00	**−0.06**	0.00	**−0.13**	**−0.06**	**−0.04**	**0.05**	**−0.28**
b.height	Z_{pbl}	−4.52	−1.01	−8.83	−1.49	−4.12	−1.34	−13.5	0.9	−9.57	**−18.9**
50 %	V_{10m}	**0.06**	−0.03	**0.11**	0.05	**0.09**	−0.02	0.01	0.01	**0.31**	**0.06**
	Q_{2m}	0.02	**0.02**	0.01	−0.00	−0.00	−0.01	**0.05**	0.00	**0.04**	**0.08**
	P_{tot}	0.39	−0.44	−0.23	0.27	**−0.40**	0.10	0.88	−0.12	0.10	0.23
SEN2	T_{2m}	0.01	**0.03**	0.02	**0.02**	−0.02	**0.01**	0.00	**0.03**	**0.08**	**0.10**
str.width	Z_{pbl}	−0.40	4.35	−13.6	3.47	4.13	**4.67**	4.93	0.84	**7.55**	**8.73**
50 %	V_{10m}	**0.06**	**0.09**	**0.10**	**0.14**	**0.12**	**0.10**	**0.05**	0.02	**0.30**	**0.31**
	Q_{2m}	−0.01	−0.00	0.01	−0.02	0.00	−0.00	0.01	0.00	**−0.05**	−0.00
	P_{tot}	0.46	−0.60	0.11	−0.03	**−0.41**	**0.29**	0.70	−0.39	−0.05	−0.07
SEN3	T_{2m}	**−0.11**	**−0.20**	**−0.11**	0.02	**−0.06**	0.01	**−0.08**	−0.01	**−0.13**	−0.00
2 x	Z_{pbl}	**−17.5**	1.11	**−31.8**	4.86	−11.0	**8.46**	**−28.7**	3.00	**−24.8**	−1.92
roof alb.	V_{10m}	−0.02	−0.03	−0.02	0.02	−0.02	−0.01	**−0.04**	−0.01	**−0.05**	−0.00
	Q_{2m}	0.02	0.02	−0.01	−0.01	**−0.05**	**−0.06**	0.03	−0.00	−0.00	0.04
	P_{tot}	0.17	**−1.00**	0.10	0.02	**−0.57**	0.36	0.56	−0.33	−0.05	−0.09
SEN4	T_{2m}	**−0.07**	−0.01	−0.05	**0.03**	−0.04	**−0.05**	**−0.1**	**−0.04**	**−0.07**	**−0.10**
AHR	Z_{pbl}	−15.6	**5.38**	8.71	5.63	−6.60	**8.57**	**−37.7**	3.15	**−17.6**	**−9.14**
50 %	V_{10m}	−0.02	0.01	−0.02	0.01	0.03	−0.02	−0.03	−0.02	0.01	**−0.05**
	Q_{2m}	**0.04**	**0.02**	**−0.00**	−0.00	−0.00	−0.02	**0.00**	**−0.02**	0.02	**0.09**
	P_{tot}	0.45	−0.37	**−1.00**	−0.17	−0.19	0.18	0.67	−0.02	**−0.59**	0.19

ACPD
14, 18541–18589, 2014

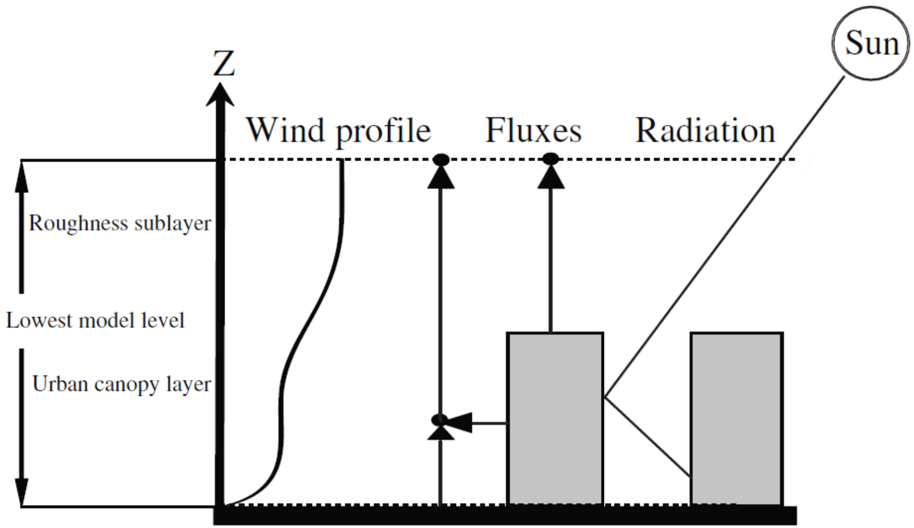

Figure 1. A schematic representation of the SLUCM (after Chen et al., 2011).

ACPD
14, 18541–18589, 2014

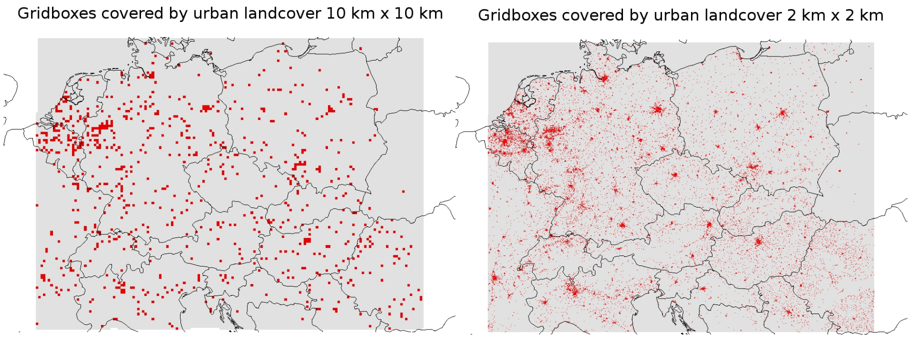

Figure 2. Urban land-surface for the 10 km × 10 km and 2 km × 2 km resolution.

Discussion Paper | Discussion Paper | Discussion Paper | Discussion Paper |

ACPD

14, 18541–18589, 2014

Urban land-surface impact on climate

P. Huszar et al.

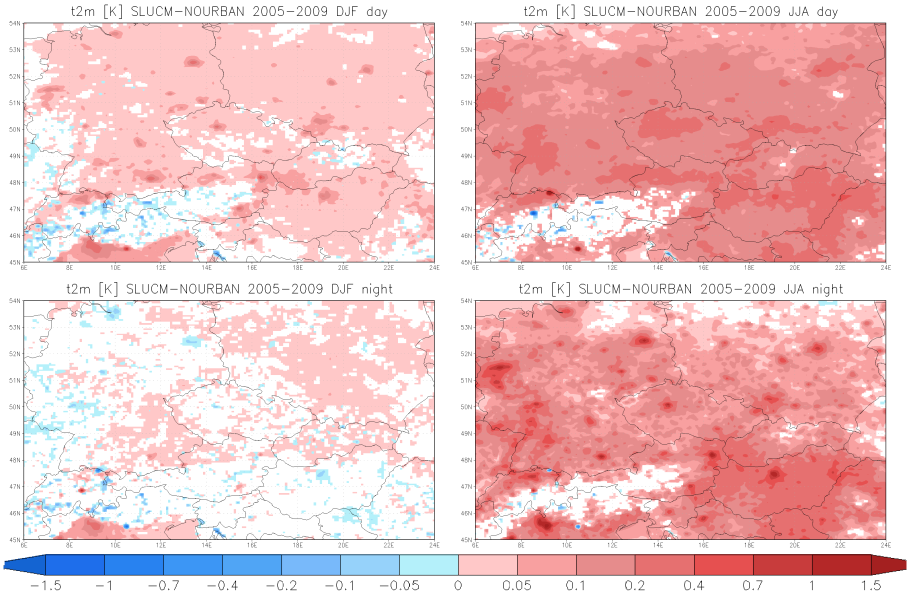

Figure 3. The impact of urbanized surfaces on the winter (left) and summer (right) near surface temperature for day (above) and night-time (bottom) conditions in K averaged over years 2005–2009. Shaded areas represent statistically significant differences on the 95 % level.

ACPD
14, 18541–18589, 2014

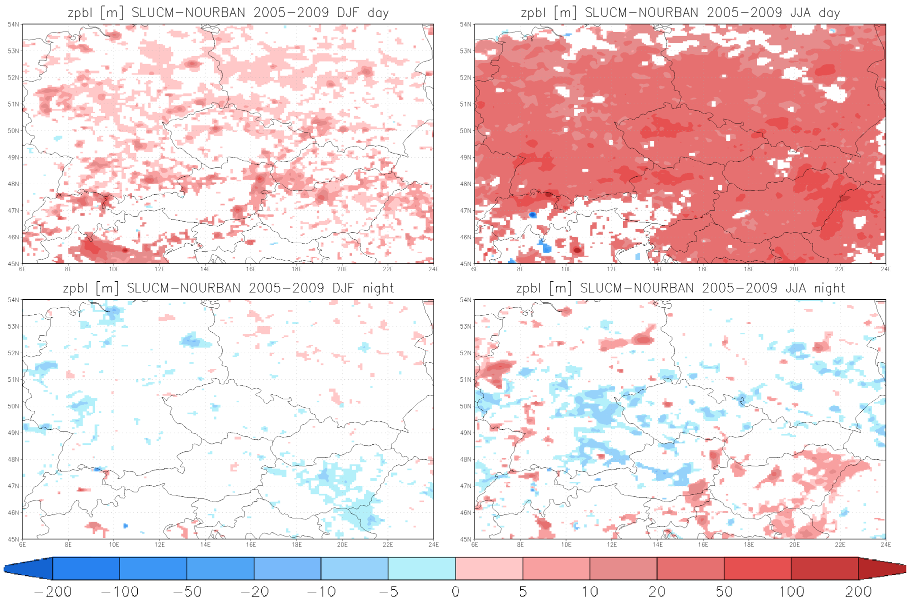

Figure 4. Same as Fig. 3 but for the PBL height in meters.

ACPD
14, 18541–18589, 2014

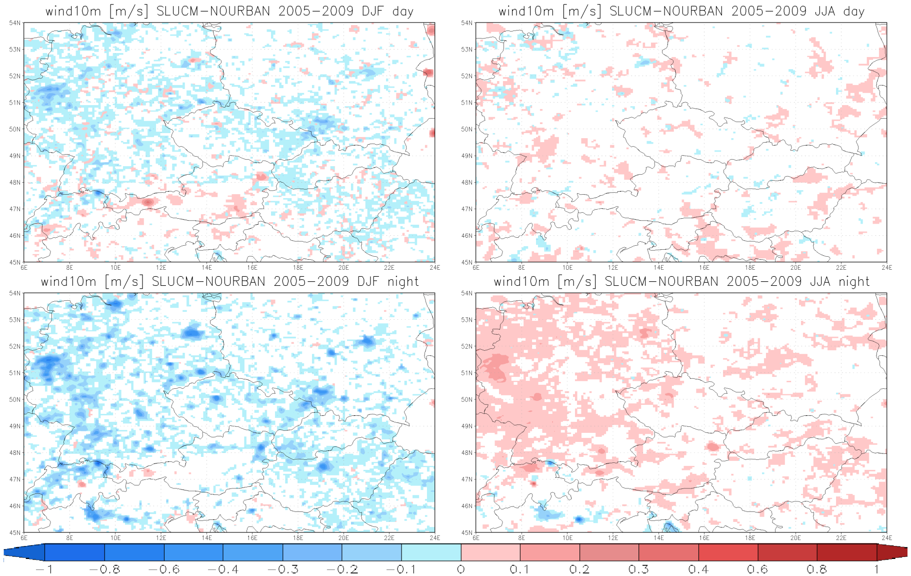

Figure 5. Same as Fig. 3 but for the wind velocity at 10 m in $m\,s^{-1}$.

ACPD
14, 18541–18589, 2014

Urban land-surface impact on climate

P. Huszar et al.

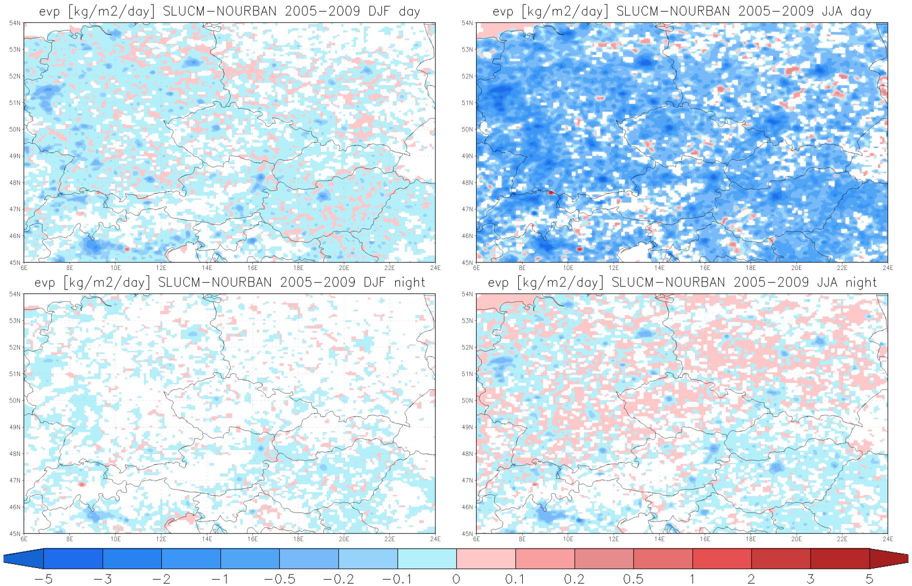

Figure 6. Same as Fig. 3 but for the surface evaporation in $kg\,m^{-2}\,day^{-1}$.

ACPD
14, 18541–18589, 2014

Urban land-surface impact on climate

P. Huszar et al.

Title Page
Abstract Introduction
Conclusions References
Tables Figures
◀I ▶I
◀ ▶
Back Close
Full Screen / Esc
Printer-friendly Version
Interactive Discussion

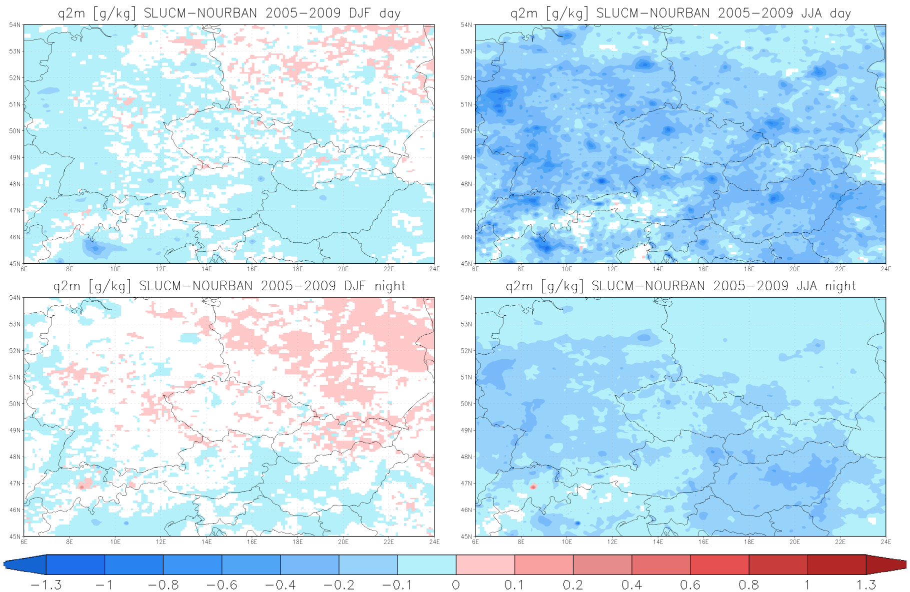

Figure 7. Same as Fig. 3 but for the surface specific humidity in $g\,kg^{-1}$.

ACPD
14, 18541–18589, 2014

Urban land-surface impact on climate

P. Huszar et al.

Title Page
Abstract Introduction
Conclusions References
Tables Figures
◄ ►
◄ ►
Back Close
Full Screen / Esc
Printer-friendly Version
Interactive Discussion

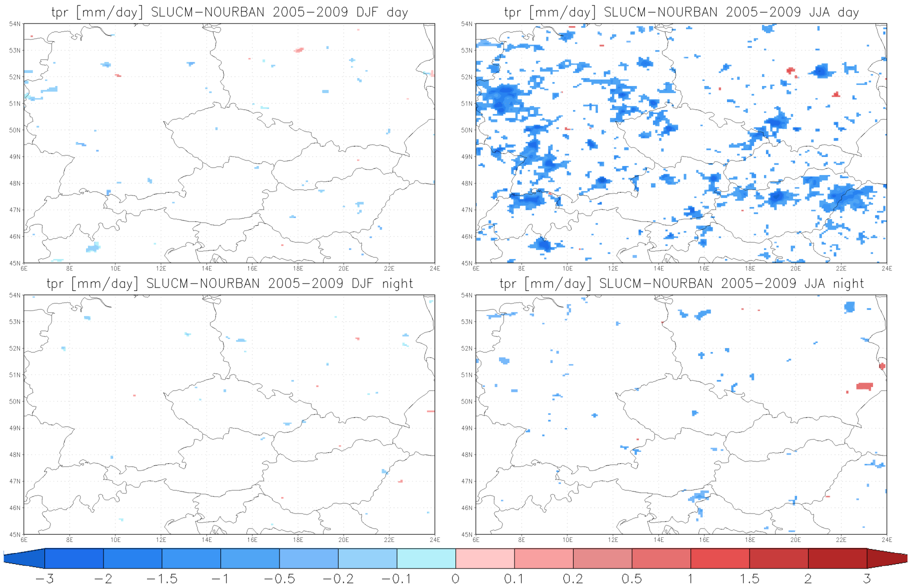

Figure 8. Same as Fig. 3 but for the total precipitation rate in mm day^{-1}.

ACPD
14, 18541–18589, 2014

Figure 9. The impact of urbanized surfaces on the winter (left) and summer (right) vertical cross-section of temperature along the 50° N latitude for day (above) and night-time (bottom) conditions in K averaged over years 2005–2009. The vertical axis denotes the average model levels heights in meters. Shaded areas represent statistically significant differences on the 95 % level.

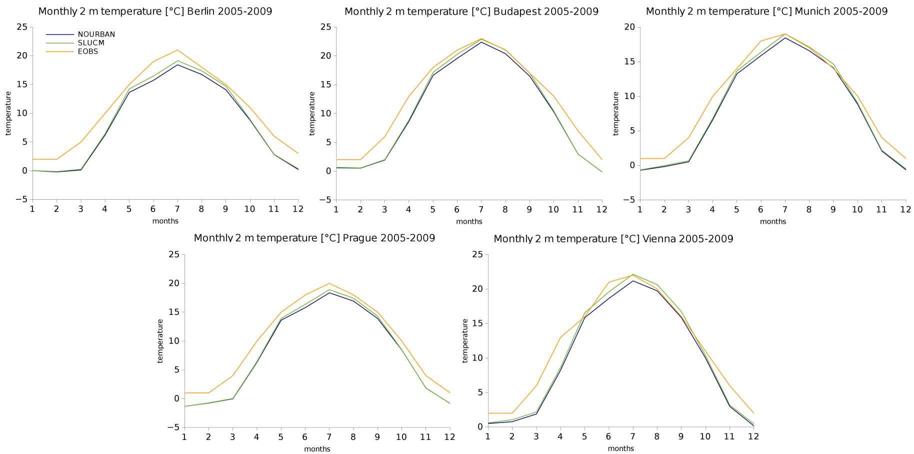

Figure 10. The mean 2005–2009 monthly 2 m temperatures averaged over selected cities in central Europe for the NOURBAN (blue), SLUCM (pink) runs and extracted from E-OBS observational data (orange).

ACPD
14, 18541–18589, 2014

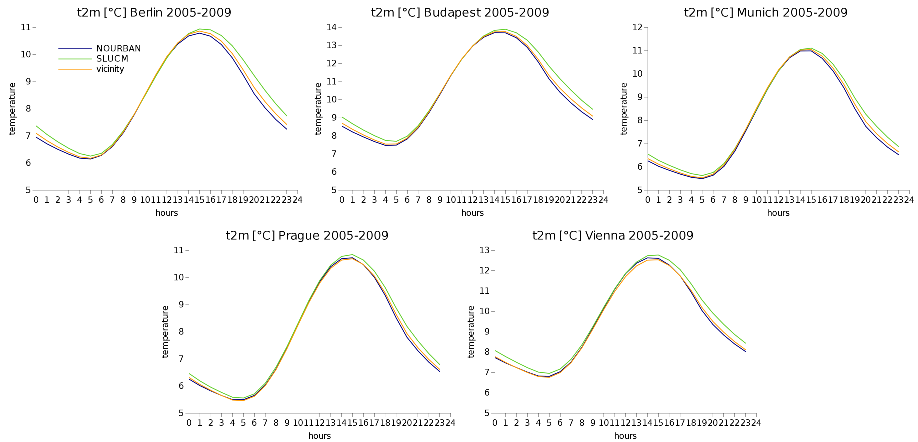

Figure 11. The mean 2005–2009 diurnal 2 m temperatures variation averaged over selected cities and over its vicinity in central Europe for the NOURBAN (blue), SLUCM (pink – city, orange – vicinity) runs.

ACPD
14, 18541–18589, 2014

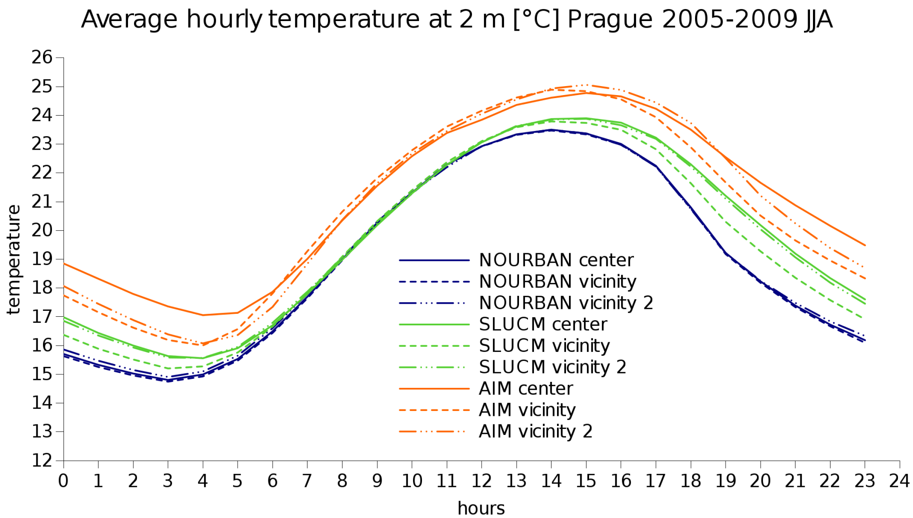

Figure 12. The mean summer diurnal 2 m temperatures variation in Prague for the NOURBAN experiment (blue), the SLUCM experiment (pink) and for measurements (orange) from a station in the center of Prague (solid line) and two stations from the vicinity of the city (dashed lines).

ACPD
14, 18541–18589, 2014

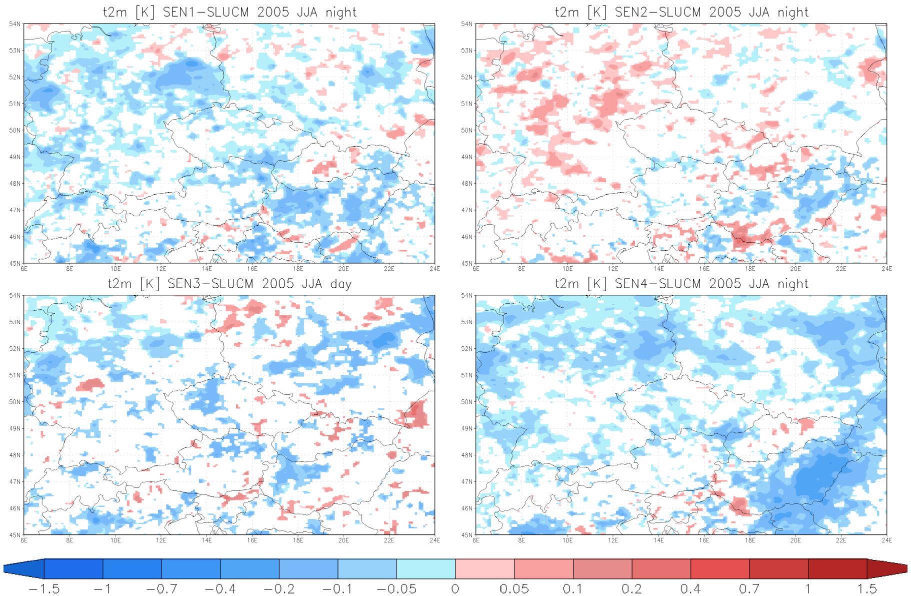

Figure 13. Sensitivity test: the impact of 50 % reduction of building size (upper left), 50 % reduction of street width (upper right), 2 times higher roof albedo (bottom left) and 50 % reduction of AHR (bottom right) on 2005 summer average near surface temperature for night-time conditions (SEN1, SEN2 and SEN4) and daytime conditions (SEN3) in K. Shaded areas represent statistically significant differences on the 95 % level.

ACPD
14, 18541–18589, 2014

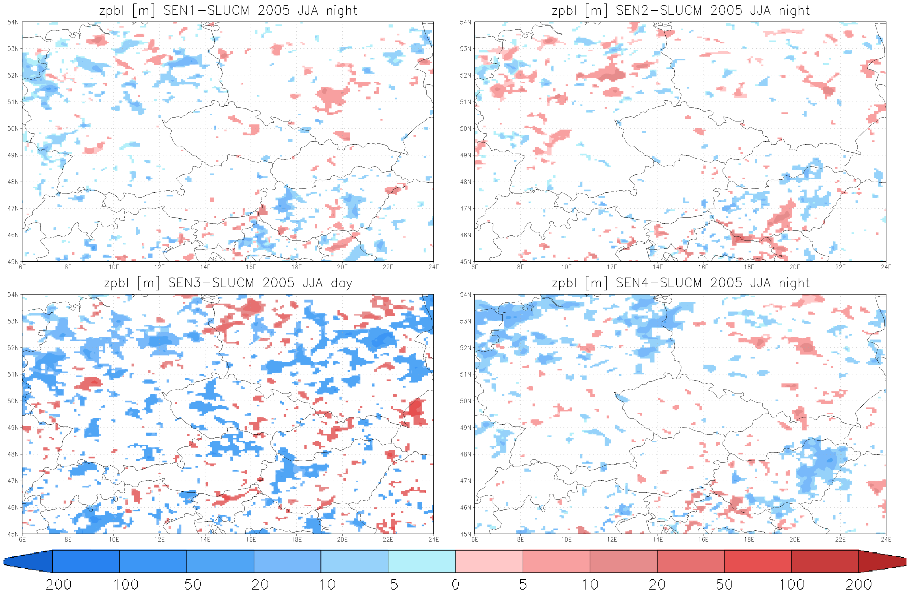

Figure 14. Same as Fig. 13 but for the PBL height in m.

Discussion Paper | Discussion Paper | Discussion Paper | Discussion Paper |

ACPD
14, 18541–18589, 2014

Urban land-surface impact on climate

P. Huszar et al.

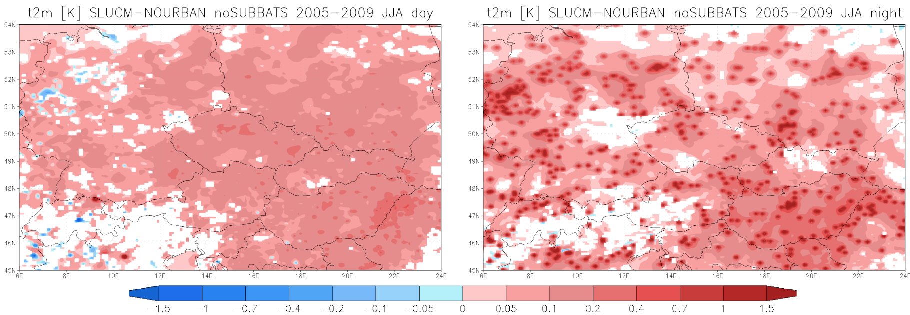

Figure 15. The impact of urbanized surfaces on the summer day (left) and night (right) near surface temperature in K averaged over years 2005–2009 without SUBBATS, i.e. at 10 km × 10 km model resolution. Shaded areas represent statistically significant differences on the 95 % level.

ACPD
14, 18541–18589, 2014

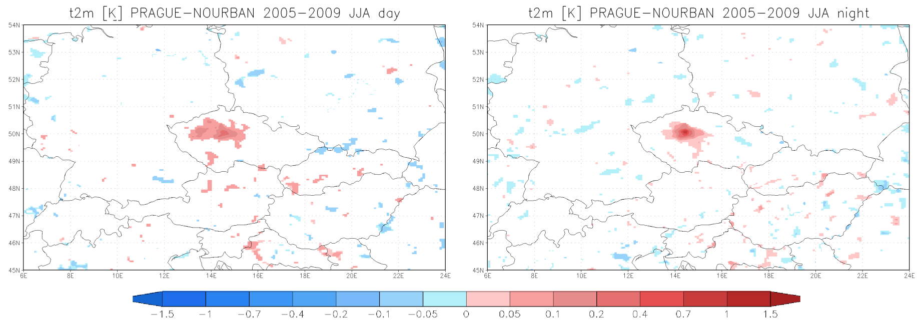

Figure 16. Impact of urbanized surfaces corresponding to Prague on the near surface temperature including the SUBBATS surface treatment (2 km × 2 km resolution). Shaded areas represent statistically significant differences on the 95 % level.

ACPD
14, 18541–18589, 2014